Modulation of the Turnover of Formamidopyrimidine DNA Glycosylase†

Michael B. Harbut,‡ Michael Meador,§ M. L. Dodson,§ and R. S. Lloyd*,‡

Center for Research on Occupational and Environmental Toxicology, Oregon Health and Science University, 3181 SW Sam Jackson Park Road, L606, Portland, Oregon 97239-3098, and Sealy Center for Molecular Science and Department of Biochemistry and Molecular Biology, The University of Texas Medical Branch, 301 University Avenue, Galveston, Texas 77555-1071

Received November 21, 2005; Revised Manuscript Received March 15, 2006

ABSTRACT: In recent years, significant progress has been made in determining the catalytic mechanisms by which base excision repair (BER) DNA glycosylases and glycosylase-abasic site (AP) lyases cleave the glycosyl bond. While these investigations have identified active site residues and active site architectures, few investigations have analyzed postincision turnover events. Previously, we identified a critical residue (His16) in the T4-pyrimidine dimer glycosylase (T4-Pdg) that, when mutated, interferes with enzyme turnover [Meador et al. (2004) *J. Biol. Chem. 279*, 3348−3353]. To test whether comparable residues and mechanisms might be operative for other BER glycosylase:AP-lyases, molecular modeling studies were conducted comparing the active site regions of T4-Pdg and the *Escherichia coli* formamidopyrimidine DNA glycosylase (Fpg). These analyses revealed that His71 in Fpg might perform a similar function to His16 in T4-Pdg. Site-directed mutagenesis of the *Fpg* gene and analyses of the reaction mechanism of the mutant enzyme revealed that the H71A enzyme retained activity on a DNA substrate containing an 8-oxo-7,8-dihydroguanine (8-oxoG) opposite cytosine and DNA containing an AP site. The H71A Fpg mutant was severely compromised in enzyme turnover on the 8-oxoG-C substrate but had turnover rates comparable to that of wild-type Fpg on AP-containing DNA. The similar mutant phenotypes for these two enzymes, despite a complete lack of structural or sequence homology between them, suggest a common mechanism for the rate-limiting step catalyzed by BER glycosylase:AP-lyases.

Prokaryotic and eukaryotic cells utilize a number of different mechanisms to repair constantly accumulating DNA damage due to environmental and endogenous chemical agents. In the absence of repair, many DNA lesions may block replication and transcription, while others may decrease replication fidelity. These disruptions may result in mutations and ultimately carcinogenesis in eukaryotes. The base excision repair (BER)[1] pathway is a key component in the cellular response to DNA lesions (*1*). Formamidopyrimidine DNA glycosylase (Fpg) functions in the *Escherichia coli* BER pathway as an *N*-glycosylase and abasic site (AP) lyase, with the predominant DNA incision product resulting from a δ-elimination reaction (*2*). The Fpg glycosylase activity results in the removal of formamidopyrimidine (Fapy) and 8-oxo-7,8-dihydroguanine (8-oxoG) lesions (*3*, *4*). The catalytic mechanism of Fpg is similar to that of other BER glycosylases that manifest an AP-lyase capability (*5*). The active site nucleophile is the N-terminal proline secondary amine (*6*). This nucleophile collapses onto C1′ of the scissile base deoxyribose moiety due to the developing electrophilic character at C1′, concomitant with the glycosylase step (ref *5* and M. L. Dodson, unpublished results).

The crystal and cocrystal structures of the *E. coli* Fpg and Fpg homologues from other bacterial and human sources have been published (*7*−*11*). Recent NMR analyses of free Fpg and Fpg bound to duplex DNA containing a site-specific AP site analogue revealed a highly dynamic structure, even in complex with DNA (*12*). These data are consistent with molecular dynamics calculations of the enzyme in complex with 8-oxoG, even though the conclusions of these investigations differed concerning the *anti/syn* conformation of a bound 8-oxoG substrate (*13*−*15*). Precatalytic and catalytic mechanisms of Fpg have also been extensively investigated (*13*, *16*−*20*). These investigations reveal a complex series of enzyme and DNA conformational changes that ultimately result in the formation of the Michaelis complex. Predictions concerning amino acid residues that could modulate precatalytic and catalytic steps based on structures, dynamics, and spectroscopy have been successfully carried out, revealing molecular details of the overall catalytic mechanism (*13*).

McCullough et al. (*5*) have discussed that the product spectra of the BER glycosylase-lyase enzymes arise as a consequence of kinetic competitions between sequential elimination events (glycosyl bond cleavage, β-elimination, δ-elimination) and hydrolysis of the corresponding covalent enzyme−product intermediates. Bhagwat and Gerlt (*21*)

† This work was supported by National Institutes of Health Grant ES04091.

* To whom correspondence should be addressed. Phone: (503) 494-9957. Fax: (503) 494-6831. E-mail: lloydst@ohsu.edu.

‡ Oregon Health and Science University.

§ University of Texas Medical Branch.

[1] Abbreviations: 8-oxoG, 8-oxo-7,8-dihydroguanine; AP, apurinic; BER, base excision repair; DTT, dithiothreitol; Fapy, formamidopyrimidine; Fpg, formamidopyrimidine DNA glycosylase; T4-Pdg, T4-pyrimidine dimer glycosylase; EDTA, ethylenediaminetetraacetic acid; PMSF, phenylmethanesulfonyl fluoride; HEPES, *N*-(2-hydroxyethyl)-piperazine-*N*′-2-ethanesulfonic acid.

10.1021/bi052383p CCC: $33.50
Published on Web 05/17/2006

demonstrated that the Fpg δ-elimination step was dependent on a prior β-elimination step, a result that supports the kinetic competition argument. One corollary of that argument is that the cleavage of the covalent product from the enzyme is rate limiting in the catalytic scheme. The predominance of the δ-elimination product is consistent with the slow hydrolysis of Schiff base intermediates involving secondary amines. It has been suggested that the conserved Glu3 residue electrostatically stabilizes the electrophilic C1′ and subsequently, the protonated Schiff base intermediate (*22*, *23*). Mutation of Lys57, whose ϵ-amine contacts the phosphates one and two nucleotides 3′ to the 8-oxoG site, abolishes activity on 8-oxoG but has little effect on AP-lyase activity (*8*, *24*). Gilboa et al. (*8*) have suggested that Lys57 protonates the leaving 3′-phosphate, thereby accelerating the β-elimination step.

Results from studies of other combined glycosylase:AP-lyases, such as T4-pyrimidine dimer glycosylase (T4-Pdg) and endonuclease VIII, may also be used to suggest key amino acid residues involved in the catalytic mechanism of Fpg, due to a commonality in catalytic mechanisms. Meador et al. (*25*) showed that mutation of the His16 residue of T4-Pdg resulted in an enzyme that was severely compromised in turnover following the catalytic events. The His16 residue had been originally hypothesized to be involved in the formation of the Schiff base or subsequent intermediates. Further investigations did not support this hypothesis. The mutant enzymes were able to carry out the glycosylase step, form the Schiff base intermediate, and carry out the lyase step. However, the rate of product formation rapidly plateaued over time and was directly proportional to the amount of enzyme added. It was concluded that the His16 residue was involved in enzyme−product turnover. The mechanistic similarities between T4-Pdg and Fpg suggested that some residue in the Fpg structure might play a role similar to that of T4-Pdg His16. This study tests that hypothesis by identifying a similar candidate histidine residue, mutating that residue, and investigating the alteration in catalytic properties of the mutant enzymes. The commonality of mutant enzyme phenotypes exists despite a complete lack of structural or sequence homology and entirely different active site architectures. The implication is that these residues catalyze the rate-limiting and essential step for these BER DNA lyases.

EXPERIMENTAL PROCEDURES

Molecular Modeling. Two structures from the Protein Data Bank were modeled, 1VAS (T4-Pdg) and 1K82, residues 1−128 (Fpg). The orientation frames for the two structures were set with a custom program written in the NAB molecular structure manipulation language (*26*). The frames were defined using the positions of the N-terminal nitrogens, the CA carbons of the histidine residues, and the CA carbons of E3 (1K82) or Q23 (1VAS). The latter two residues (E23 in wild-type 1VAS) are key catalytic species and are thought to play similar roles in the catalytic schemes of Fpg and T4-Pdg, respectively. The molecular graphics were generated with MOLSCRIPT (*27*) and Raster3D (*28*).

Targeted Mutagenesis of the E. coli Fpg Protein. In vitro mutagenesis was performed using bidirectional polymerase chain reaction. Histidine-71 was changed to alanine (GCT). The mutagenesis was verified via DNA sequencing at the University of Texas Medical Branch NIEHS Molecular Biology Core. The pTYBII-Fpg H71A plasmid encoding the mutant Fpg protein was transformed into *E. coli* CC104 (*mutM*$^-$) DE3 cells.

Expression and Purification of the H71A Mutant Fpg Protein. The expression and purification of the mutant Fpg proteins were performed using the New England BioLabs Impact T7 protein expression and purification system. A culture of CC104 (*mutM*$^-$) cells carrying the pTYBII-Fpg H71A plasmid was grown in Luria broth supplemented with 100 μg/mL ampicillin at 37 °C to an $OD_{600\ nm}$ of 0.5. Protein expression was induced for 2.5 h at 37 °C by the addition of isopropyl β-D-thiogalactopyranoside to 0.3 mM final concentration. Cells were harvested by centrifugation and resuspended in 50 mM HEPES, pH 7.5, 500 mM NaCl, 1 mM ethylenediaminetetraacetic acid, 0.1 mM phenylmethanesulfonyl flouride, and 1:20 (v/v) of protease inhibitor (Sigma). The cells were broken by sonication on ice. Clarified extracts were prepared by centrifugation at 10000 rpm for 10 min. Polymin P (Sigma) (10% w/v) was slowly added to the clarified extracts (over 30 min) with constant stirring to a final concentration of 0.1%. The Polymin P precipitate was removed by centrifugation at 10000 rpm for 10 min. Ammonium sulfate was slowly added to the supernatants (over 30 min) with constant stirring to achieve 60% saturation. The resulting precipitated proteins were collected by centrifugation as described above and resuspended in 10 mL of 50 mM HEPES, pH 7.5, 1 mM EDTA and 0.1 mM PMSF. A 15 mL chitin affinity column was washed with 10 column volumes of buffer A (50 mM Na-HEPES, pH 7.5 1 M NaCl, 1 mM EDTA, and 0.1 mM PMSF). The proteins were loaded onto the column, and the column was washed with 20 column volumes of the buffer A, followed by a 15 min wash of 3 column volumes of buffer A containing 50 mM dithiothreitol (DTT). The proteins were left on the column overnight at 4 °C and then eluted with buffer B (25 mM Na-HEPES, pH 7.5, 1 M NaCl, and 1 mM EDTA) and collected in 1 mL fractions. Aliquots of the fractions were analyzed on a 10% SDS−polyacrylamide gel. The pure protein-containing fractions were dialyzed into 25 mM Na-HEPES, 250 mM NaCl, 1 mM EDTA, 1 mM DTT, 1 mM PMSF, and 50% glycerol, separated into aliquots, and stored at −20 °C. Protein concentration was determined using the Bradford method (Bio-Rad).

Activity of Fpg on an 8-Oxoguanine-Containing DNA Substrate. An oligodeoxynucleotide with the sequence 5′-ACCATGCCTGCACGACOAAAGCAATTCGTA-3′, where O denotes 8-oxoG, and its complement 5′-TACGAAT-TGCTTTCGTCGTGCAGGCATGGT-3′ were synthesized by Midland Certified Reagent Co. (Midland, TX). The 8-oxoG-containing oligodeoxynucleotide was ^{32}P labeled at its 5′ end with T4 polynucleotide kinase (New England BioLabs) and annealed to its complementary strand. Fpg enzymes were incubated at 37 °C with the double-stranded 30-mer 8-oxoG DNA (4.5 nM) in a reaction containing 25 mM Na-HEPES, pH 7.5, 50 mM NaCl, 2 mM EDTA, 1 mM DTT, and 0.1 mg/mL BSA. Aliquots (10 μL) were quenched with an equal volume of loading buffer: 95% (v/v) formamide, 20 mM EDTA, 0.02% (w/v) bromphenol blue, and 0.02% (w/v) xylene cyanol. The aliquots were heated at 90 °C for 5 min prior to being loaded on a 15% polyacrylamide

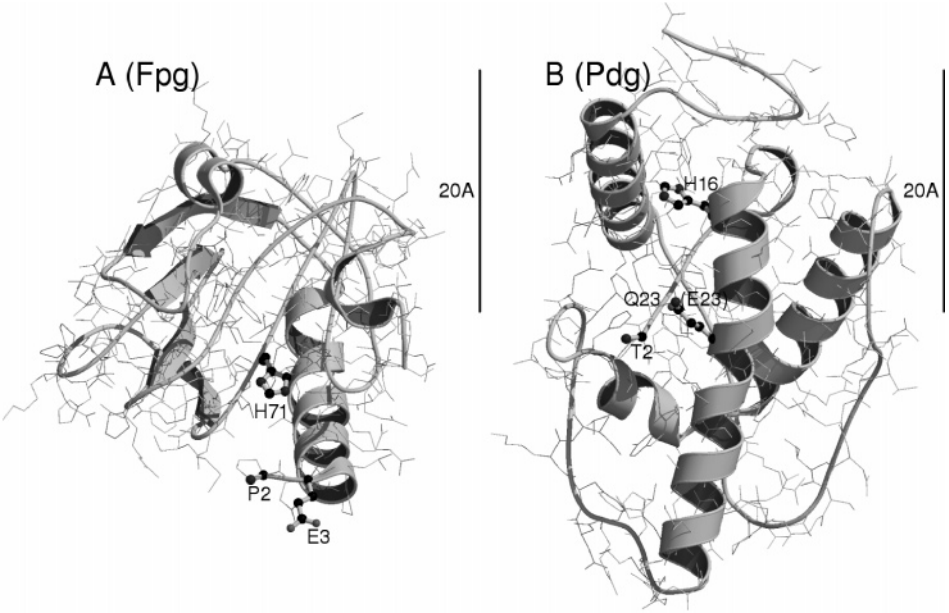

FIGURE 1: Geometric relationships between key residues in T4-Pdg and Fpg (residues 1−128). Panel A (Fpg): Residues 1−128 of the Protein Data Bank entry 1K82 oriented such that the triangle formed by the N-terminal proline nitrogen, the H71 CA carbon, and the E3 CA carbon lies in the plane of the paper, with the horizontal axis defined by the line between the proline nitrogen and the E3 CA carbon. The vertical axis is defined by the right-hand vector cross-product in the plane of the paper and orthogonal to the horizontal axis. Panel B (Pdg): The PDB entry 1VAS is shown oriented similarly to Fpg in panel A. The triangle formed by the N-terminal nitrogen, the H16 CA carbon, and the Q23 CA carbon (E23 in the wild-type enzyme) lies in the plane of the paper, and the horizontal axis is defined by the N-terminal threonine nitrogen and the Q23 CA carbon. The vertical axis is defined as the vector cross-product as in panel A. In both panels the histidine residue is at the top vertex of the triangle. The key residue side chains are represented as balls and sticks, colored according to atom type, and labeled. The bars at the right sides of the two panels represent 20 Å.

gel (8 M urea) in 0.5 × TBE buffer. The DNA substrates and products were separated by electrophoresis for 2 h at 20 W, and the gels were visualized and analyzed with PhophorImager screens and ImagQuant 5.2 software (Amersham Biosciences).

Activity of Fpg on DNA Containing an AP Site. A 25-mer oligodeoxynucleotide with the sequence 5′-CGATAGT-GTCCAUGTTACTCGAAGC-3′ and its complement 5′-GCTTCGAGTAACGTGGACACTATCG-3′ were synthesized by Midland Certified Reagent Co. and 5′-^{32}P labeled. An AP site was produced by treating 4.5 nM annealed 25-mer with 2 units of uracil DNA glycosylase (New England BioLabs) in 20 mM Tris-HCl pH 7.5, 1 mM DTT, and 1 mM EDTA for 25 min at 37 °C. Fpg enzymes were incubated with the AP-containing DNA immediately thereafter, and 10 μL aliquots were removed at the indicated time points and treated with freshly prepared 200 mM $NaBH_4$ for 2 min. Loading buffer was added to the aliquots analyzed as described above, with the trapped complexes migrating into the gel but significantly slower than that of the substrate and product DNA.

Formation of Covalent Enzyme−DNA Complexes Using $NaBH_4$. To reduce Schiff base intermediates between the Fpg enzymes and substrate DNA, $NaBH_4$ was added to a final concentration of 100 mM from a freshly prepared 1 M stock solution simultaneously with the DNA substrates. These reactions were incubated at 37 °C for 30 min, an equal amount of formamide loading buffer was added, and the samples analyzed as previously described. When carried out with an excess of DNA substrate, the fraction of DNA molecules forming a covalent intermediate, as measured by the gel migration pattern characteristic of covalent protein−DNA complexes [Meador et al. (*25*)], should directly measure the active molecules in the enzyme preparation. Burst kinetics methods for determining the fraction of active enzyme molecules would be problematic since the apparent defect in the H71A mutant was in the turnover step. However, actual results obtained in this investigation reveal difficulties with the borohydride trapping procedure, and these will be discussed in the Results section.

RESULTS

Molecular Modeling. The crystal structure of *E. coli* Fpg was examined for histidine residues that might be similar in their geometric relationships to His16 in T4-Pdg. The distances between the amine nitrogens of the N-terminal residues and the centers of mass of the histidine imidazoles were measured in the two structures. The center of mass of the imidazole ring of the His71 residue in Fpg was 9.0 Å from the N-terminal proline nitrogen, whereas the center of mass of the imidazole of the His16 residue was 12.5 Å from the N-terminal threonine nitrogen in T4-Pdg. If the structure of T4-Pdg was taken as represented in the unpublished structure of a borohydride-reduced imine DNA−enzyme intermediate instead of that in 1VAS, the center of mass of the His16 imidazole ring was 11.4 Å from the N-terminal nitrogen (Gali Golan, Dmitry O. Zharkov, Gil Shoham, Arthur P. Grollman, M. L. Dodson, Amanda K. McCullough, and R. Stephen Lloyd, submitted for publication). His71 seemed the most likely candidate and so was chosen for mutational alteration. Figure 1 shows the geometric relationships between three key residues in (A) Fpg, residues 1−128, and (B) T4-Pdg. The bar on the right side of both panels represents 20 Å.

Activity on an 8-Oxoguanine-Containing Substrate. The mutant H71A Fpg protein was assayed for activity on

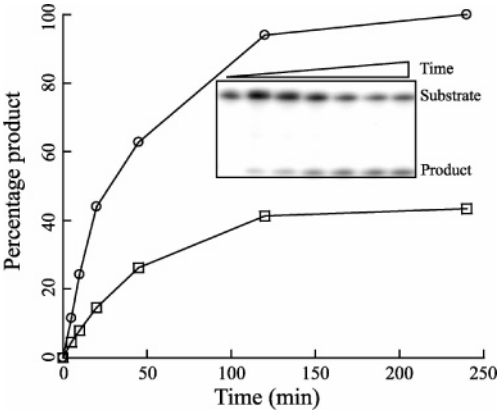

FIGURE 2: Wild-type and H71A Fpg enzyme kinetics on 8-oxoguanine-containing DNA. Substrate oligodeoxynucleotides containing 8-oxoG were treated with equal total molar concentrations of wild-type (○) or H71A (□) Fpg as described in the Experimental Procedures. The kinetics of product accumulation are shown in which the DNA concentration was 4.5 nM, and the apparent active protein concentrations were 185 pM for H71A and 681 pM for WT. Aliquots were removed at 5, 10, 20, 45, 120, and 240 min. Also shown is a storage phosphor autoradiogram of a representative H71A (185 pM) time course assay on 8-oxoG-containing DNA (4.5 nM). The first lane contained no enzyme. From left to right, the lanes after the first correspond to time points of 5, 10, 20, 45, 120, and 240 min. The total concentration of WT = 12 nM and H71A = 12 nM.

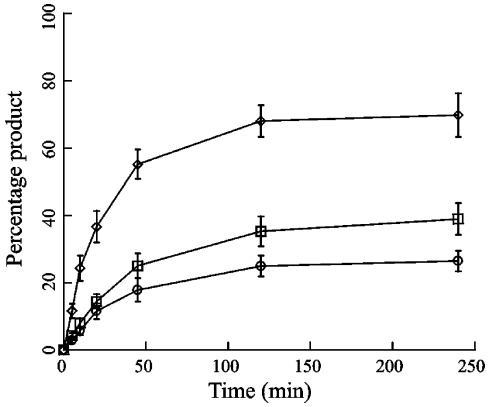

FIGURE 3: Incision kinetics of H71A Fpg at varied enzyme protein concentrations on duplex DNA containing 8-oxoguanine−cytosine. The kinetics of incised product accumulation are shown as a percentage of total substrate DNA in which the DNA concentration was held constant at 4.5 nM, and the apparent active enzyme concentrations were varied: 92.5 pM (○), 185 pM (□), and 370 pM (◇). Results of four independent experiments are given as the mean values ± SD. Aliquots were removed at 5, 10, 20, 45, 120, and 240 min. The total concentration of H71A = 6, 12, and 24 nM.

substrate DNA containing an 8-oxoG−cytosine base pair centrally located in the duplex DNA. The data in Figure 2 show the ability of equal total concentrations (cf. Experimental Procedures) of the mutant H71A and wild-type Fpg to incise the duplex substrate DNA at the site of the 8-oxoG. Although the initial rate of incision by the mutant was somewhat lower, the accumulation of incised DNA products from reaction with the H71A mutant enzyme dramatically slows down over the course of the assay and reached a plateau value, less than complete conversion of substrate to product. To rule out the possibility that the mutant H71A enzyme was losing activity during the kinetic analyses, reactions containing all components except the 8-oxoG-containing substrate DNA were incubated for 1 h at 37 °C before the addition of labeled substrate DNA. The initial reaction rates were identical to those without preincubation at 37 °C, ruling out the explanation that the enzyme rapidly lost activity at 37 °C.

Since these data were collected using equal total concentrations of wild-type and mutant enzymes, separate experiments were carried out to determine the relative fraction of active enzyme molecules in each preparation. Active site titrations were performed using $NaBH_4$ reduction of the Schiff base intermediates formed between the N-terminal proline secondary amine and C1′ of the substrate site deoxyribose. Enzyme concentrations were adjusted such that less than 30% of the input labeled 8-oxoG containing DNA was trapped as a covalent complex. These data showed that the purified wild-type enzyme contained 3−4-fold more active molecules when compared to the H71A mutant (data not shown). In light of these data, the adjusted rates of incision for the data in Figure 2 showed approximately equal catalytic efficiency.

The borohydride trapping method for active site titration carries the implicit assumption that the imine intermediate to be reduced is accessible to the borohydride in solution. To the extent that this assumption is not satisfied, the trapping method will underestimate the fraction of molecules that are active. Figure 2 shows a plateau for the H71A mutant at approximately 40% of the input DNA substrate (4.5 nM). The straightforward interpretation of this is that the H71A mutant produced 1.8 nM (40% of 4.5 nM) imine intermediate DNA, at variance with the expected activity from the borohydride trapping experiments. The activity observed in Figure 2 should, therefore, be taken as an upper bound of the activity of the mutant enzyme, with the activity measured in the borohydride trapping experiment taken as a lower bound. Due to these uncertainties in the true fractions of active enzyme in the preparations, the active enzyme concentrations reported in the figure legends are referred to as "apparent active enzyme concentrations".

To determine whether the plateau value of the H71A Fpg was proportional to the amount of enzyme added, the enzyme concentration was varied over a 4-fold range. These data (Figure 3) show that the accumulation of DNA product plateaus at values proportional to the input enzyme concentration. Since Fpg has both DNA glycosylase and AP-lyase activities, it was possible that the H71A mutation might have uncoupled the glycosylase step from the (obligatorily subsequent) lyase event. To test this possibility, kinetic reactions were treated (or not) with hot piperidine to cleave DNA with AP sites. Incubation of H71A Fpg-treated DNA with piperidine showed no difference in the amount of cleavage of DNA product relative to H71A Fpg-treated DNA that had not been treated with piperidine (data not shown). These data rule out an uncoupling of the reaction steps.

The data presented above were consistent with an interpretation that the H71A Fpg mutant was defective in enzyme turnover, similar to that previously observed for the T4-Pdg H16 mutants (*25*). To investigate this hypothesis, and to ensure that all 8-oxoG-containing substrates were accessible and could be cleaved by competent enzymes, duplex oligonucleotide DNAs containing 8-oxoG were incubated with either 681 pM wild-type Fpg (■) or 185 pM H71A Fpg

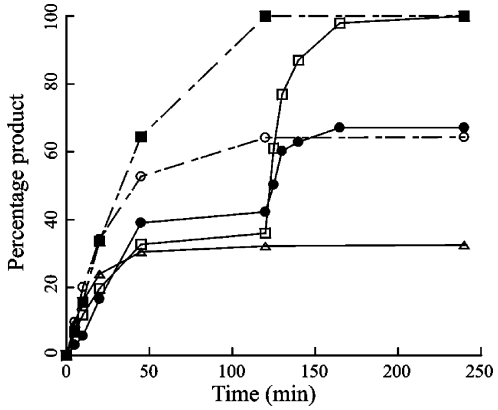

FIGURE 4: Kinetics of sequential enzyme addition. DNA containing 8-oxoG (4.5 nM) was incubated with H71A Fpg at apparent active enzyme concentrations of 185 pM (△, □, ●) or 370 pM (○) for an initial 120 min. [All enzyme concentrations reported are apparent active enzyme concentrations (cf. Experimental Procedures).] At 120 min, either 185 pM H71A (●) or 681 pM wild-type Fpg (□) was added to the reactions. No additional enzyme was added to the 185 or 370 pM H71A Fpg reactions (△ or ○, respectively). Control reactions containing wild-type Fpg at 681 pM (■) and 4.5 nM DNA were performed. The total concentration of WT = 12 nM and H71A = 12 nM.

(△, □, ●) for 120 min (Figure 4). Although the wild-type Fpg resulted in complete conversion to nicked products (■), the accumulation of incised DNA products for the first 120 min in all reactions containing the H71A Fpg reached a plateau at ∼35% conversion (△, □, ●). After 120 min an additional 185 pM H71A Fpg was introduced (●) to one of the H71A Fpg reactions, and to another, 681 pM wild-type Fpg was added (□). The product accumulation in the H71A reaction that did not receive any additional enzymes remained constant for the final 120 min reaction (△). In the H71A reaction to which additional wild-type Fpg was added, the remaining substrate DNA was rapidly incised to completion (□). The addition of another aliquot of H71A Fpg at the 120 min time point produced another burst of product that reached a plateau at ∼65% (●). An identical plateau of conversion of substrate to product was measured for H71A Fpg being added at an initial 370 pM concentration (○). Collectively, these data provide support for the hypothesis that the H71A Fpg mutant was defective in some aspect of enzyme turnover.

Kinetics with an AP Site Substrate. Although the data described above demonstrated a defective turnover for H71A Fpg on 8-oxoG substrates, all AP lyases should be capable of catalyzing a β-elimination backbone cleavage reaction on AP site-containing substrate DNA. Thus, the activity of H71A relative to the wild-type Fpg was assayed with an AP site substrate. To establish a concentration with which to carry out AP nicking, we examined a range of enzyme concentrations to empirically determine the concentration that would result in less than 50% conversion of substrate to product within 20 min. In contrast to the data previously obtained with 8-oxoG site-containing substrate DNA, H71A cleaved AP sites at a rate similar to that of wild-type Fpg (when normalized for the fraction of apparent active molecules; Figure 5) without a detectable plateau in product formation. In data not shown increased concentrations of wild-type or H71A enzymes achieved a complete conversion of substrate to product without any detectable lag.

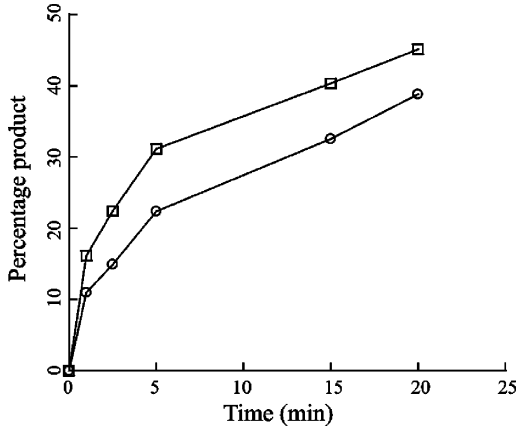

FIGURE 5: Activities of H71A and wild-type Fpg on an AP site-containing substrate. A substrate oligodeoxynucleotide containing an AP site (4.5 nM) was treated with wild-type or H71A Fpg as described in the Experimental Procedures. The kinetics of the production of incised DNA molecules for wild-type Fpg (340.5 pM apparent active enzyme protein) (□) and H71A Fpg (370 pM enzyme protein) (○). Thus, approximately equal molar apparent active enzyme concentrations of wild-type and mutant enzymes are shown. Aliquots were removed at 1, 2.5, 5, 10, and 20 min. The total concentration of WT = 6 nM and H71A = 24 nM.

DISCUSSION

Data presented herein provide evidence for a role of His71 in facilitating the turnover of Fpg acting on an 8-oxoG-containing duplex DNA. The Fpg active site is located in a cleft between two domains, and the active site residues are located on one surface of this cleft (Figure 1, panel A). The scissile substrate nucleotide is flipped into the active site in the Michaelis complex. If the substrate is Fapy or 8-oxoG in the context of duplex DNA, water is likely to be excluded from the active site, but if the substrate is an AP site, the volume ordinarily occupied by the flipped base should be filled with water molecules. Since the δ-elimination product is the most frequently accumulated product species prior to enzyme−product turnover, the enzyme is covalently bound to a 5-carbon fragment derived from the deoxyribose of the scissile base (*21*). The gapped DNA product is free to dissociate. Hydrolysis of the 5-carbon sugar fragment imine should be rate limiting for enzyme turnover (*5*).

Mutation of His71 prevents enzyme turnover, directly implicating this residue in the hydrolysis of the enzyme:5-carbon sugar fragment imine product. The role of this residue is probably to act as a general base activating a water molecule for the hydrolysis (*29*). If dissociation of the scissile base from the active site pocket were prevented by the product imine, turnover in the mutant enzyme would be prevented. In the case of the δ-elimination product being generated by the reaction at an AP site, water trapped in the scissile base pocket should be able to hydrolyze the imine product by attack on the imine from within the pocket. We suggest that this scenario explains the difference in mutant enzyme turnover when the enzyme is acting on an 8-oxoG versus an AP site substrate.

In conclusion, the histidine at sequence position 71 has been shown to be an essential residue for the biologically required turnover of the Fpg AP-lyase covalent enzyme−product species. Since these two enzymes share no sequence homology and completely differ in the base-flipping schemes used to form their respective Michaelis complexes, yet share

a (apparently convergent) scheme for turnover of their covalent imine product complexes, these results strongly suggest a generalization to BER glycosylase:AP-lyase enzymes. The general base residue need not be a histidine, but we suggest that the structure of all such enzymes will reveal a similarly placed residue with a similar catalytic potential (activation of the hydrolytic water molecule).

ACKNOWLEDGMENT

We thank Dr. Amanda K. McCullough for helpful discussions and Toni Brennan for manuscript preparation.

REFERENCES

1. Sancar, A., Lindsey-Boltz, L. A., Unsal-Kacmaz, K., and Linn, S. (2004) Molecular mechanisms of mammalian DNA repair and the DNA damage checkpoints, *Annu. Rev. Biochem. 73*, 39−85.
2. Bailly, V., Verly, W. G., O'Connor, T., and Laval, J. (1989) Mechanism of DNA strand nicking at apurinic/apyrimidinic sites by *Escherichia coli* [formamidopyrimidine]DNA glycosylase, *Biochem. J. 262*, 581−589.
3. Tchou, J., Kasai, H., Shibutani, S., Chung, M. H., Laval, J., Grollman, A. P., and Nishimura, S. (1991) 8-oxoguanine (8-hydroxyguanine) DNA glycosylase and its substrate specificity, *Proc. Natl. Acad. Sci. U.S.A. 88*, 4690−4694.
4. Chetsanga, C. J., and Lindahl, T. (1979) Release of 7-methylguanine residues whose imidazole rings have been opened from damaged DNA by a DNA glycosylase from *Escherichia coli*, *Nucleic Acids Res. 6*, 3673−3684.
5. McCullough, A. K., Dodson, M. L., and Lloyd, R. S. (1999) Initiation of base excision repair: glycosylase mechanisms and structures, *Annu. Rev. Biochem. 68*, 255−285.
6. Zharkov, D. O., Rieger, R. A., Iden, C. R., and Grollman, A. P. (1997) NH_2-terminal proline acts as a nucleophile in the glycosylase/AP-lyase reaction catalyzed by *Escherichia coli* formamidopyrimidine-DNA glycosylase (Fpg) protein, *J. Biol. Chem. 272*, 5335−5341.
7. Zharkov, D. O., Golan, G., Gilboa, R., Fernandes, A. S., Gerchman, S. E., Kycia, J. H., Rieger, R. A., Grollman, A. P., and Shoham, G. (2002) Structural analysis of an *Escherichia coli* endonuclease VIII covalent reaction intermediate, *EMBO J. 21*, 789−800.
8. Gilboa, R., Zharkov, D. O., Golan, G., Fernandes, A. S., Gerchman, S. E., Matz, E., Kycia, J. H., Grollman, A. P., and Shoham, G. (2002) Structure of formamidopyrimidine-DNA glycosylase covalently complexed to DNA, *J. Biol. Chem. 277*, 19811−19816.
9. Sugahara, M., Mikawa, T., Kumasaka, T., Yamamoto, M., Kato, R., Fukuyama, K., Inoue, Y., and Kuramitsu, S. (2000) Crystal structure of a repair enzyme of oxidatively damaged DNA, MutM (Fpg), from an extreme thermophile, *Thermus thermophilus* HB8, *EMBO J. 19*, 3857−3869.
10. Fromme, J. C., and Verdine, G. L. (2002) Structural insights into lesion recognition and repair by the bacterial 8-oxoguanine DNA glycosylase MutM, *Nat. Struct. Biol. 9*, 544−552.
11. Serre, L., Pereira de Jesus, K., Boiteux, S., Zelwer, C., and Castaing, B. (2002) Crystal structure of the *Lactococcus lactis* formamidopyrimidine-DNA glycosylase bound to an abasic site analogue-containing DNA, *EMBO J. 21*, 2854−2865.
12. Buchko, G. W., McAteer, K., Wallace, S. S., and Kennedy, M. A. (2005) Solution-state NMR investigation of DNA binding interactions in *Escherichia coli* formamidopyrimidine-DNA glycosylase (Fpg): a dynamic description of the DNA/protein interface, *DNA Repair (Amsterdam) 4*, 327−339.
13. Zaika, E. I., Perlow, R. A., Matz, E., Broyde, S., Gilboa, R., Grollman, A. P., and Zharkov, D. O. (2004) Substrate discrimination by formamidopyrimidine-DNA glycosylase: a mutational analysis, *J. Biol. Chem. 279*, 4849−4861.
14. Amara, P., Serre, L., Castaing, B., and Thomas, A. (2004) Insights into the DNA repair process by the formamidopyrimidine-DNA glycosylase investigated by molecular dynamics, *Protein Sci. 13*, 2009−2021.
15. Perlow-Poehnelt, R. A., Zharkov, D. O., Grollman, A. P., and Broyde, S. (2004) Substrate discrimination by formamidopyrimidine-DNA glycosylase: distinguishing interactions within the active site, *Biochemistry 43*, 16092−16105.
16. Tchou, J., Bodepudi, V., Shibutani, S., Antoshechkin, I., Miller, J., Grollman, A. P., and Johnson, F. (1994) Substrate specificity of Fpg protein. Recognition and cleavage of oxidatively damaged DNA, *J. Biol. Chem. 269*, 15318−15324.
17. Ishchenko, A. A., Vasilenko, N. L., Sinitsina, O. I., Yamkovoy, V. I., Fedorova, O. S., Douglas, K. T., and Nevinsky, G. A. (2002) Thermodynamic, kinetic, and structural basis for recognition and repair of 8-oxoguanine in DNA by Fpg protein from *Escherichia coli*, *Biochemistry 41*, 7540−7548.
18. Fedorova, O. S., Nevinsky, G. A., Koval, V. V., Ishchenko, A. A., Vasilenko, N. L., and Douglas, K. T. (2002) Stopped-flow kinetic studies of the interaction between *Escherichia coli* Fpg protein and DNA substrates, *Biochemistry 41*, 1520−1528.
19. Zharkov, D. O., Shoham, G., and Grollman, A. P. (2003) Structural characterization of the Fpg family of DNA glycosylases, *DNA Repair (Amsterdam) 2*, 839−862.
20. Koval, V. V., Kuznetsov, N. A., Zharkov, D. O., Ishchenko, A. A., Douglas, K. T., Nevinsky, G. A., and Fedorova, O. S. (2004) Pre-steady-state kinetics shows differences in processing of various DNA lesions by *Escherichia coli* formamidopyrimidine-DNA glycosylase, *Nucleic Acids Res. 32*, 926−935.
21. Bhagwat, M., and Gerlt, J. A. (1996) 3′- and 5′-strand cleavage reactions catalyzed by the Fpg protein from *Escherichia coli* occur via successive beta- and delta-elimination mechanisms, respectively, *Biochemistry 35*, 659−665.
22. Lavrukhin, O. V., and Lloyd, R. S. (2000) Involvement of phylogenetically conserved acidic amino acid residues in catalysis by an oxidative DNA damage enzyme formamidopyrimidine glycosylase, *Biochemistry 39*, 15266−15271.
23. Burgess, S., Jaruga, P., Dodson, M. L., Dizdaroglu, M., and Lloyd, R. S. (2002) Determination of active site residues in *Escherichia coli* endonuclease VIII, *J. Biol. Chem. 277*, 2938−2944.
24. Sidorkina, O. M., and Laval, J. (1998) Role of lysine-57 in the catalytic activities of *Escherichia coli* formamidopyrimidine-DNA glycosylase (Fpg protein), *Nucleic Acids Res. 26*, 5351−5357.
25. Meador, M. G., Rajagopalan, L., Lloyd, R. S., and Dodson, M. L. (2004) Role of His-16 in turnover of T4 pyrimidine dimer glycosylase, *J. Biol. Chem. 279*, 3348−3353.
26. Macke, T., and Case, D. A. (1998) in *Molecular Modeling of Nucleic Acids* (Leontes, N. B., and J. SantaLucia, J., Eds.) pp 379−393, American Chemical Society, Washington, DC.
27. Kraulis, P. (1991) MOLSCRIPT: a program to produce both detailed and schematic plots of protein structures, *J. Appl. Crystallogr. 24*, 946−950.
28. Merritt, E. A., and Bacon, D. J. (1997) Raster3D: Photorealistic molecular graphics, *Methods Emzymol. 277*, 505−524.
29. Jencks, W. P. (1996) *Catalysis in Chemistry and Enzymology*, Dover Publications, New York.

BI052383P